

First Structurally Characterized Tricyanomanganate(III) and its Magnetic $\{Mn^{III}_2M^{II}_2\}$ Complexes ($M^{II} = Mn, Ni$)

Minao Tang,[†] Dongfeng Li,^{†,‡} Uma Prasad Mallik,[#] Jeffrey R. Withers,[#] Shari Brauer,[#] Michael R. Rhodes,[#] Rodolphe Clérac,^{*,§,||} Gordon T. Yee,[⊥] Myung-Hwan Whangbo,^{||} and Stephen M. Holmes^{*,†,‡}

[†]Department of Chemistry, University of Kentucky, Lexington, Kentucky, 40506-0055, [‡]Key Laboratory of Pesticide and Chemical Biology of Ministry of Education, College of Chemistry, Central China Normal University, 430079 Wuhan, China, [§]CNRS, UPR 8641, Centre de Recherche Paul Pascal (CRPP), 115 avenue du Dr. Albert Schweitzer, Pessac, F-33600, France, ^{||}Université de Bordeaux, UPR 8641, Pessac, F-33600, France, [⊥]Department of Chemistry, Virginia Polytechnic Institute and State University, Blacksburg, Virginia 24061, and ^{||}Department of Chemistry, North Carolina State University, Raleigh, North Carolina 27695-8204. [#]Current address: Department of Chemistry & Biochemistry, University of Missouri-St. Louis, St. Louis, Missouri 63121.

Received April 7, 2010

Treatment of tris(3-cyano-2,4-pentanedionato)manganese(III) with KTp^{*}, followed by [NEt₄]CN affords [NEt₄][(Tp^{*})Mn^{III}(CN)₃] (**1**); subsequent treatment of **1** with divalent triflates (OTf) and 2,2'-bipyridine (bpy) affords $\{Mn^{III}_2M^{II}_2\}$ complexes ($M^{II} = Mn, Ni$, **3**). Magnetic measurements show that **1–3** exhibit $S_T = 1, 3$, and 4 spin ground states, respectively.

Cyanometalates find extensive use as reagents for the rational construction of polynuclear complexes that exhibit superparamagnetism like behavior,¹ spin crossover,^{2a} and optically responsive materials.^{2b,c} Using a synthetic strategy known as a building block approach, molecular precursors are allowed to self-assemble with intact structures into a common structural archetype. The most common units for constructing polynuclear cyanometalate complexes are those containing tripodal ligands, L, with generalized $[fac-LM^II(CN)_m]_{1,2a-c}$ stoichiometry.

Over the last five years, we have systematically investigated the use of poly(pyrazolyl)borates as platforms for tuning the magnetic and optical behavior of several structurally related

tri-, tetra-, and octanuclear complexes. Tricyano- building blocks such as [(Tp^R)Fe^{III}(CN)₃][−] (Tp^R = pzTp, Tp, Tp^{*}) exhibit substantial orbital contributions to their $S_T = 1/2$ ground state that are crucial for engineering polynuclear complexes that exhibit slow relaxation of the magnetization (i.e., single-molecule magnets, SMMs).^{1d-i}

In oxo-carboxylate complex chemistry, high spin ($S = 2$) manganese(III) ions are used extensively as a source of single-ion magnetic anisotropy in the design of SMMs.^{2d} However, surprisingly few cyanomanganate analogues have been described with the best characterized example being a pentanuclear complex containing [Mn^{II}(tmphen)]²⁺ (tmphen = 3,4,7,8-tetramethyl-1,10-phenanthroline) and hexacyanomanganate(III) ions in a 3:2 ratio;^{1b,2a} this trigonal bipyramidal complex exhibits slow dynamics below 1.8 K (for a time scale of 1 s). Surprisingly, however, no tricyano- analogues have been reported to date. In the present Communication, we describe the synthesis of the first tricyanomanganate(III) complex and its self-assembly into well-defined $\{Mn^{III}_2M^{II}_2\}$ complexes.

Treatment of tris(3-cyano-2,4-pentanedionato)manganese(III) with KTp^{*} followed by three equivalents of [NEt₄]CN in methanol affords [NEt₄][(Tp^{*})Mn(CN)₃] (**1**) as yellow crystals.³ The infrared spectrum of **1** contains intense $\tilde{\nu}_{BH}$

*To whom correspondence should be addressed. E-mail: holmesst@umsl.edu (S.M.H.); clerac@crpp-bordeaux.cnrs.fr (R.C.).

(1) (a) Sokol, J. J.; Hee, A. G.; Long, J. R. *J. Am. Chem. Soc.* **2002**, *124*, 7656–7657. (b) Berlinguette, C. P.; Vaughn, D.; Cañada-Vilalta, C.; Galán-Mascarós, J. R.; Dunbar, K. R. *Angew. Chem., Int. Ed.* **2003**, *43*, 1606–1608. (c) Schelter, E. J.; Prosvirin, A. V.; Dunbar, K. R. *J. Am. Chem. Soc.* **2004**, *126*, 15004–15005. (d) Li, D.; Parkin, S.; Wang, G.; Yee, G. T.; Clérac, R.; Wernsdorfer, W.; Holmes, S. M. *J. Am. Chem. Soc.* **2006**, *128*, 4214–4215. (e) Li, D.; Parkin, S.; Wang, G.; Yee, G. T.; Prosvirin, A. V.; Holmes, S. M. *Inorg. Chem.* **2005**, *44*, 4903–4905. (f) Li, D.; Clérac, R.; Parkin, S.; Wang, G.; Yee, G. T.; Holmes, S. M. *Inorg. Chem.* **2006**, *45*, 4307–4309. (g) Kim, J.; Han, S.; Cho, I.-K.; Chi, K. Y.; Heu, M.; Yoon, S.; Suh, B. *J. Polyhedron* **2004**, *23*, 1333–1339. (h) Wang, S.; Zuo, J.-L.; Zhou, H.-C.; Choi, H. J.; Ke, Y.; Long, J. R.; You, X.-Z. *Angew. Chem., Int. Ed.* **2002**, *124*, 7656–7657. (i) Wang, S.; Zuo, J.-L.; Zhou, H.-C.; Song, Y.; Gao, S.; You, X.-Z. *Eur. J. Inorg. Chem.* **2004**, 3681–3687.

(2) (a) Funck, K. E.; Hilfiger, M. G.; Berlinguette, C. P.; Shatruk, M.; Wernsdorfer, W.; Dunbar, K. R. *Inorg. Chem.* **2009**, *48*, 3438–3452 and references cited therein. (b) Sato, O.; Tao, J.; Zhang, Y.-Z. *Angew. Chem., Int. Ed.* **2007**, *46*, 2152–2187 and references cited therein. (c) Li, D.; Clérac, R.; Roubeau, O.; Harté, E.; Mathonière, C.; Le Bris, R.; Holmes, S. M. *J. Am. Chem. Soc.* **2008**, *130*, 252–258. (d) Sessoli, R.; Gatteschi, D. *Angew. Chem., Int. Ed.* **2003**, *42*, 268–297.

(3) (a) See the Supporting Information. (b) Crystal data for **1**: C₂₆H₄₂BMnN₁₀P₃, Z = 3, a = 9.8102(1) Å, b = 9.8102(1) Å, c = 26.2483(4) Å, V = 2187.70(5) Å³, R₁ = 0.0427, wR₂ = 0.0800. Crystal data for **2**: C₇₈H₇₈B₂Mn₄N₂₆O₇S₂, P₁, Z = 2, a = 13.431(1) Å, b = 18.332(2) Å, c = 19.943(2) Å, α = 88.878(5)°, β = 89.742(5)°, γ = 74.204(5)°, V = 4724.1(8) Å³, R₁ = 0.0977, wR₂ = 0.1886.

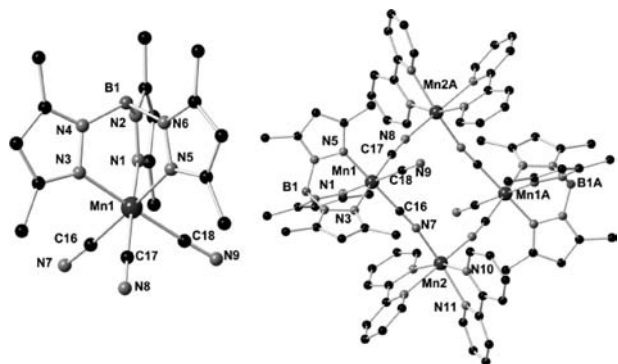


Figure 1. X-ray structures of **1** (left) and **2** (right). All cations, anions, lattice solvents, and hydrogen atoms are eliminated for clarity.

and $\tilde{\nu}_{\text{CN}}$ stretches [2552 and 2113 cm^{-1}] that are shifted to higher energies relative to KTP^* (2436 cm^{-1}) and $[\text{NET}_4]\text{CN}$ (2056 cm^{-1}), respectively.^{4a,b} For **1**, the $\tilde{\nu}_{\text{CN}}$ stretch is higher in energy than those seen for $[\text{Mn}^{\text{II}}(\text{CN})_2(\text{bpy})_2] \cdot 3\text{H}_2\text{O}$ (2114 cm^{-1}), $[\text{NET}_4]_2[\text{Mn}^{\text{II}}(\text{CN})_4]$ (2120 and 2078 cm^{-1}), $\text{K}_3[\text{Mn}^{\text{III}}(\text{CN})_6] \cdot \text{H}_2\text{O}$ (2112 and 2121 cm^{-1}), $[\text{NET}_4]_3[\text{Mn}^{\text{III}}(\text{CN})_6] \cdot \text{H}_2\text{O}$ (2094 cm^{-1}), and $[\text{PPN}]_3[\text{Mn}^{\text{III}}(\text{CN})_6]$ (2096 cm^{-1}), suggesting that charge delocalization (via π -back bonding) is less efficient.^{3a,4b–g,5a}

Treatment of **1** with a 1:2 ratio of $\text{Mn}(\text{OTf})_2$ and bpy or $[\text{Ni}(\text{bpy})_2(\text{OH}_2)_2](\text{OTf})_2$ in acetonitrile readily affords $[(\text{Tp}^*)\text{Mn}^{\text{III}}(\text{CN})_3]_2[\text{M}^{\text{II}}(\text{bpy})_2](\text{OTf})_2 \cdot n\text{H}_2\text{O}$ ($\text{M}^{\text{II}} = \text{Mn}$, **2**; Ni , **3**). The energies of the $\tilde{\nu}_{\text{CN}}$ stretches in **2** and **3** are similar to those reported for $\{\text{Mn}^{\text{III}}_2\text{Mn}^{\text{II}}_3\}$ [2068–2138 cm^{-1}] and $\text{Ni}^{\text{II}}_3[\text{Mn}^{\text{III}}(\text{CN})_6] \cdot 12\text{H}_2\text{O}$ [2164 cm^{-1}], while intense $\tilde{\nu}_{\text{BH}}$ [2551 and 2552 cm^{-1}] absorptions are comparable to those found in infrared spectra of **1**. We conclude that $\text{Mn}^{\text{III}}(\mu\text{-CN})\text{M}^{\text{II}}$ linkages are present in **2** and **3**.^{3a,4c,5a}

Compound **1** crystallizes in the trigonal $P3_2$ space group.^{3b} The C_{3v} -symmetric anions have Mn–C and Mn–N distances that range between 1.976(3) and 1.985(3) Å and 2.019(2) and 2.036(2) Å, respectively, indicating that no Jahn–Teller distortions are present (Figure 1 and Supporting Information Figure S2). In **1**, the average Mn–C distances [1.976(3) Å] are comparable to those in $\text{K}_3[\text{Mn}^{\text{III}}(\text{CN})_6]$ [1.978(2) Å] and $[\text{PPN}]_3[\text{Mn}(\text{CN})_6]$ [2.020(2) Å], while the C–Mn–C angles are between 85.8(1)° [C17–Mn1–C18] and 91.7(1)° [C16–Mn1–C18]; the N–Mn–N angles are between 87.56(8)° [N3–Mn1–N5] and 89.65(9)° [N1–Mn1–N5].^{3a,5a,5b} Close $\text{Tp}^*\text{-Tp}^*$ methyl [3.596(3) Å] and cyanide–methyl contacts [3.452(3) Å] are also present in structures of **1** (Supporting Information Figures S3–S4).^{3a}

(4) (a) Andreades, S.; Zahnow, E. W. *J. Am. Chem. Soc.* **1969**, *91*, 4181–4190. (b) Trofimenko, S.; Long, J. R.; Nappier, T.; Shore, S. G. *Inorg. Synth.* **1970**, *12*, 99–107. (c) Smith, J. A.; Galán-Mascarós, J. R.; Clérac, R.; Sun, J.-S.; Ouyang, X.; Dunbar, K. R. *Polyhedron* **2001**, *20*, 1727–1734. (d) Buschmann, W. E.; Liable-Sands, L.; Rheingold, A. L.; Miller, J. S. *Inorg. Chim. Acta* **1999**, *284*, 175–179. (e) Manson, J. L.; Buschmann, W. E.; Miller, J. S. *Inorg. Chem.* **2001**, *40*, 1926–1935. (f) Qureshi, A. M.; Sharpe, A. G. *J. Inorg. Nucl. Chem.* **1968**, *30*, 2269–2270. (g) Buschmann, W. E.; Arif, A. M.; Miller, J. S. *Angew. Chem., Int. Ed.* **1998**, *37*, 781–783.

(5) (a) Nakamoto, K. *Infrared and Raman Spectra of Inorganic and Coordination Compounds*, 5th ed., Part B; Wiley: New York, 1977. (b) Gupta, M. P.; Milledge, H. J.; McCarthy, A. E. *Acta Crystallogr.* **1974**, *B30*, 656–661. (c) Li, D.; Parkin, S.; Wang, G.; Yee, G. T.; Holmes, S. M. *Inorg. Chem.* **2006**, *45*, 5251–5253. (d) Li, D.; Clérac, R.; Wang, G.; Yee, G. T.; Holmes, S. M. *Eur. J. Inorg. Chem.* **2007**, 1341–1346. (e) Kambe, K. *J. Phys. Soc. Jpn.* **1950**, *5*, 48–51. (f) Li, D.; Parkin, S.; Wang, G.; Yee, G. T.; Holmes, S. M. *Inorg. Chem.* **2006**, *45*, 1951–1959. (g) Borrás-Alemenar, J. J.; Clemente-Juan, J. M.; Coronado, E.; Tsukerblat, B. S. *J. Comput. Chem.* **2001**, *22*, 985–991.

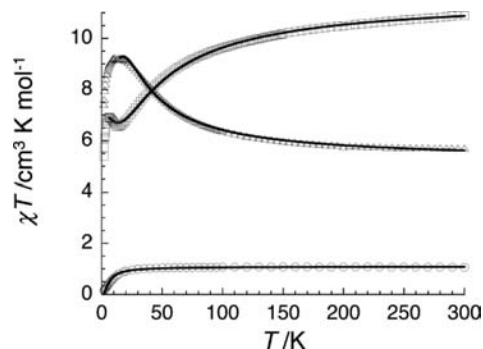


Figure 2. χT vs T plots for **1** (○), **2** (□), and **3** (△) at $H_{\text{dc}} = 1000$ Oe (χ being the magnetic susceptibility defined as M/H per complex). The solid black lines are the best fit and simulations obtained (see text).

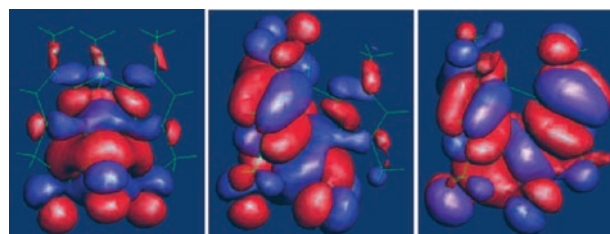


Figure 3. Shapes of the three lowest energy orbitals of **1** obtained from EHTB calculations: (left) $d(z^2)$, (middle) $d(xz)$, and (right) $d(yz)$ orbitals.

Crystals of **2** are found in the $P\bar{1}$ space group and its tetranuclear core consists of alternating di- and trivalent manganese ions linked by cyanides.^{3a,b} The Mn^{III} centers (Mn1 and Mn1A) contain terminal cyanides (C18–N9) that are related via inversion centers and adopt an anti orientation relative to the $\{\text{Mn}^{\text{III}}_2(\mu\text{-CN})_4\text{Mn}^{\text{II}}_2\}$ plane (Figure 1 and Supporting Information Figures S5–S7). Complex **2** is structurally related to $\{\text{Fe}^{\text{III}}_2\text{M}^{\text{II}}_2\}$ and $\{[\text{V}^{\text{IV}}\text{O}]_2\text{Mn}^{\text{II}}_2\}$ analogues where a Tp^* methyl projects toward the rectangular face that is opposite to the terminal cyanide.^{5c,d} The $\{\text{Mn}^{\text{III}}_2\text{Mn}^{\text{II}}_2\}$ core is slightly larger than the corresponding Fe^{III} analogues due to longer average Mn1–C [1.970(6) Å] and Mn2–N [2.154(5) Å] bonds; close bpy– Tp^* ring contacts [3.185(3) Å] are also present.^{3a}

At 300 K, the χT product of **1** is 1.1 $\text{cm}^3 \text{K mol}^{-1}$, which is in good agreement with the expected value (1.0 $\text{cm}^3 \text{K mol}^{-1}$) for a complex containing a magnetically isolated Mn^{III} ion with two unpaired electrons (Figure 2). On the other hand, the experimental χT value is far from those seen for either $[\text{PPN}]_2[\text{Mn}^{\text{II}}(\text{CN})_4]$ or $[\text{PPN}]_3[\text{Mn}^{\text{III}}(\text{CN})_6]$ (4.49 and 1.98 $\text{cm}^3 \text{K mol}^{-1}$), suggesting that trivalent ions are present and that orbital contributions to the spin ground state are nearly absent in **1**.^{3a,4d–g} At low temperatures, the χT product follows Curie behavior down to 100 K and then decreases toward a minimum value of 0.15 $\text{cm}^3 \text{K mol}^{-1}$ at 1.8 K. To reproduce this thermal behavior, an anisotropic Heisenberg Hamiltonian ($H = D S_{\text{Mn}}^2$) was utilized; the calculated values for g and D/k_B are 2.09(2) and +9.4(2) K, respectively (Figure 2 and Supporting Information Figure S8).^{3a} The surprisingly large value of D must be considered with caution as antiferromagnetic intercomplex interactions probably act to artificially enhance the estimated value. This assumption is qualitatively supported by the M versus H data (below 8 K, Supporting Information Figure S9) in that the same D value was not reproduced using an anisotropic Heisenberg model.^{3a}

Extended Hückel tight-binding (EHTB) calculations⁶ for **1** suggest that it adopts an $S_T = 1$ spin ground state, because the $d(xz)$ and $d(yz)$ orbitals lie close to the $d(z^2)$ orbital (225 and 267 meV above, respectively). The shapes of these orbitals (Figure 3) show that significant π -type spin density is delocalized into the Tp* and cyanide ligands. Furthermore, short $H \cdots H$ and $H \cdots NC-Mn$ contacts (ca. 2.4 and 2.7 Å) are found between adjacent $[(Tp^*)Mn(CN)_3]^-$ anions in **1**. Below ca. 20 K these short contacts may allow for intercomplex antiferromagnetic interactions that are, as suspected (vide supra), partially responsible for the low temperature behavior of the χT data seen for **1**.

For **2**, the room temperature χT value, $10.9 \text{ cm}^3 \text{ K mol}^{-1}$, is close to that expected ($10.75 \text{ cm}^3 \text{ K mol}^{-1}$) for a $\{Mn^{III}_2Mn^{II}_2\}$ complex containing noninteracting Mn^{III} [$S = 1$, $C = 1.0 \text{ cm}^3 \text{ K mol}^{-1}$] and Mn^{II} [$S = 5/2$, $C = 4.375 \text{ cm}^3 \text{ K mol}^{-1}$] spins (Figure 2 and Supporting Information S10). At lower temperatures the χT values slowly decrease toward a minimum of $6.5 \text{ cm}^3 \text{ K mol}^{-1}$ at 14 K and below this temperature, χT increases, reaching a maximum of $6.9 \text{ cm}^3 \text{ K mol}^{-1}$ at 6 K. This thermal behavior indicates that antiferromagnetic interactions are dominant within the tetranuclear complex between adjacent $S = 1$ Mn^{III} and $S = 5/2$ Mn^{II} spins. At lower temperatures, the χT value decreases and reaches $5.2 \text{ cm}^3 \text{ K mol}^{-1}$ at 1.85 K, suggesting the presence of magnetic anisotropy and/or intercomplex antiferromagnetic interactions. On the basis of the molecular structure of **2**, the magnetic data were first modeled using an isotropic spin Hamiltonian [$H = -2J(S_1 \cdot S_2 + S_2 \cdot S_3 + S_3 \cdot S_4 + S_4 \cdot S_1)$] (eq 1), where J is the average exchange constant in the tetranuclear unit and S_i are the spin operators for the respective manganese ions [$S_1 = S_3 = S_{Mn(III)} = 1$; $S_2 = S_4 = S_{Mn(II)} = 5/2$].^{5c} MAGPACK^{5f} simulation of the experimental data above 6 K gave a rough estimation of J/k_B at $-4.8(1)$ K with $g(Mn^{II}) = 2.10(2)$ and $g(Mn^{III}) = 1.98(2)$ (Figure 2 and Supporting Information Figure S10), and this simple model leads to an energy difference between the $S_T = 3$ ground and $S_T = 2$ first excited states of ca. 19.2 K. Attempts to model the magnetic data with more parameters such as magnetic anisotropic or/and intercomplex interactions were not able to improve significantly the fit of the experimental data below 6 K. The M versus H data support an $S_T = 3$ ground state for **2** as the magnetization is almost saturated at 7 T and 1.8 K and reaches $6.3 \mu_B$ (Supporting Information Figure S11).^{3a} Additionally, **2** does not exhibit slow relaxation of its magnetization above 1.8 K, as judged from the lack of hysteresis in the M versus H (Supporting Information Figure S10) and frequency-independent ac susceptibility data in stark contrast to many reports on $S = 2$ Mn^{III} -based SMMs. We infer that the tricyanomanganate(III) ions do not bring enough magnetic anisotropy to complex **2** for the observation of SMM behavior.

The χT product at 300 K of **3** is equal to $5.4 \text{ cm}^3 \text{ K mol}^{-1}$ (Figure 2 and Supporting Information Figure S12). This value is greater than the value anticipated for isolated Mn^{III} and Ni^{II} spins ($4 \text{ cm}^3 \text{ K mol}^{-1}$ with $g = 2.0$). With decreasing temperature, the experimental χT product increases monotonically approaching a maximum of $9.2 \text{ cm}^3 \text{ K mol}^{-1}$ at 14 K.

The large room temperature χT product and its thermal behavior indicate that ferromagnetic interactions are present in **3**. Below 14 K, the χT values decrease toward a minimum of $7.4 \text{ cm}^3 \text{ K mol}^{-1}$ at 1.85 K (Figure 2),^{3a} suggesting that additional antiferromagnetic intercomplex interactions or/and magnetic anisotropy are present.

The magnetic data for **3** were also modeled using the Heisenberg Hamiltonian given in eq 1 with $S_i = S_{Mn(III)} = S_{Ni(II)} = 1$. The susceptibility was derived from application of the van Vleck equation to the Kambe vector coupling method.^{5e,f} The data fitted well to ca. 25 K with $J/k_B = +6.8(5)$ K, and $g = 2.3(1)$. Alternative models have been tried and additional intercomplex interactions treated in terms of the mean field theory were added to the Heisenberg tetranuclear model. Above 12 K, a good fit of the data is obtained and values of $J/k_B = +9.0(2)$ K, $zJ'/k_B = -0.38(5)$ K and $g = 2.3(1)$ are found (Figure 2 and Supporting Information S12).^{3a} Introduction of an anisotropic term, $2D(S_z^2(Ni) + S_z^2(Mn))$, into the Heisenberg Hamiltonian (eq 1) was also tried and the susceptibility was calculated using the MAGPACK program.^{5g} Simulations of the χT versus T data between 1.8 and 300 K have been unsuccessful, suggesting that magnetic anisotropy and intercomplex antiferromagnetic interactions are likely present in **3**. Nevertheless, the χT versus T data demonstrate the presence of ferromagnetic interactions between $S = 1$ Mn^{III} and $S = 1$ Ni^{II} spins suggesting that **3** exhibits an $S_T = 4$ ground state. At 1.8 K and $H_{dc} = 7$ T, the magnetization value ($7.1 \mu_B$) approaches that expected for an $S_T = 4$ ground state ($8 \mu_B$) (Supporting Information Figure S13). Evidence for slow relaxation of the magnetization in **3** was absent in the M versus H and ac susceptibility data above 1.8 K, suggesting misalignment of anisotropy tensors is operative in **3**.^{3a}

In summary we have described the preparation, crystal structures, and magnetic properties of a new paramagnetic tricyanomanganate(III) and two of its tetranuclear $\{Mn^{III}_2Mn^{II}_2\}$ complexes. We have shown that the $[(Tp^*)Mn^{III}(CN)_3]^-$ unit possesses an $S_T = 1$ spin state that antiferromagnetically and ferromagnetically interacts with $S = 5/2$ Mn^{II} and $S = 1$ Ni^{II} spin centers, respectively. While slow dynamics are seen for Fe^{III} analogues of **3**, $[(Tp^*)Fe^{III}(CN)_3]_2[Ni^{II}(bpy)_2]_2[OTf]_2 \cdot 2H_2O$,^{5d} the weaker magnetic anisotropy of the $[(Tp^*)Mn^{III}(CN)_3]^-$ unit leads to $S_T = 3$ and $S_T = 4$ complexes without SMM properties.

Acknowledgment. S.M.H. gratefully acknowledges the NSF (CAREER, CHE-0914935) and the University of Missouri-St. Louis for financial support. G.T.Y. acknowledges Virginia Tech and the NSF (CHE-023488) for partial support for the purchase of a Quantum Design magnetometer. M.H.W. acknowledges the U.S. DOE (DE-FG02-86ER45259). R.C. thanks the University of Bordeaux, the ANR (NT09_469563, AC-MAGnets), the Région Aquitaine, the GIS Advanced Materials in Aquitaine (COMET Project), MAGMANet (NMP3-CT-2005-515767), and the CNRS (PICS No. 4659) for support.

Supporting Information Available: Synthetic details ($[NiEt_4]_3[Mn(CN)_6]$, **1–3**) and X-ray crystallographic (CIF format, **1,2**) and additional magnetic data (Figures S1–S6). This material is available free of charge via the Internet at <http://pubs.acs.org>.

(6) (a) Calculations were carried out using the SAMOA package (<http://chvamw.chem.ncsu.edu/>). (b) Hoffman, R. J. *J. Chem. Phys.* **1963**, *39*, 1397.